Bull. Astr. Soc. India (2010) **38**, 137–145

Evaporation of extrasolar planets

A. Lecavelier des Etangs[1]*
[1]*Institut d'astrophysique de Paris, CNRS/UPMC, 98bis bld Arago, F-75014 Paris, France*

Received 2010 November 25; accepted 2010 December 02

Abstract. This article presents a review on the observations and theoretical modeling of the evaporation of extrasolar planets. The observations and the resulting constraints on the upper atmosphere (thermosphere and exosphere) of the "hot-Jupiters" are described. The early observations of the first discovered transiting extrasolar planet, HD209458b, allowed the discovery that this planet has an extended atmosphere of escaping hydrogen. Subsequent observations showed the presence of oxygen and carbon at very high altitude. These observations give unique constraints on the escape rate and mechanism in the atmosphere of hot-Jupiters. The most recent Lyman-alpha HST observations of HD189733b and MgII observations of Wasp-12b allow for the first time a comparison of the evaporation from different planets in different environments. Models to quantify the escape rate from the measured occultation depths, and an energy diagram to describe the evaporation state of hot-Jupiters are presented. Using this diagram, it is shown that few already known planets like GJ876d or CoRot-7b could be remnants of formerly giant planets.

Keywords : Planetary systems – stars: individual (HD 189733, HD 209458)

1. Rising temperature in the upper atmosphere: the thermosphere

Physical parameters of the upper atmospheres of extrasolar planets up to the exosphere (the so-called thermosphere) can be determined using absorption spectroscopy of transits. This technique has been developed in detail for HD 209458 b (Sing et al. 2008a, 2008b; Désert et al. 2008) where the detailed Temperature-Pressure-altitude profile has been estimated from ∼0.1 mbar to ∼50 mbar. In particular, because the atmospheric scale height is directly related to the temperature, the temperature can be easily determined by measurement of variation of transit occultation

*e-mail:lecaveli@iap.fr

depth as a function of wavelength. For instance, when detected the slope of absorption as a function of wavelength due to the Rayleigh scattering allows a direct determination of the temperature at the altitude where Rayleigh scattering is optically thick (Lecavelier des Etangs et al. 2008a, 2008b).

The absorption profile of sodium has been recently solved by Vidal-Madjar et al. (2011) to further constrain the vertical structure of the HD 209458b atmosphere over an altitude range of more than 6 500 km, corresponding to a pressure range of 14 scale heights spanning 1 mbar to 10^{-9} bar pressures. They found a rise in temperature above 3 mbar pressure level, and above an isothermal atmospheric layer spanning almost 6 scale heights in altitude a sharp rising of the temperature to about 2 500 K at $\sim 10^{-9}$ bar showing the presence of a thermosphere from which the gas can escape into the exosphere (Vidal-Madjar et al. 2011).

2. HD 209458 b, an evaporating planet

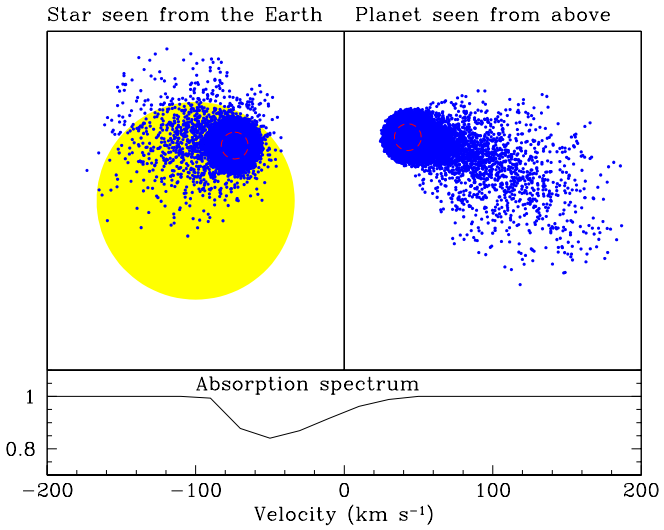

Figure 1. A numerical simulation of hydrogen atoms sensitive to radiation pressure (0.7 times the stellar gravitation) above an altitude of 0.5 times the Roche radius where the density is assumed to be 2×10^5 cm^{-3} is presented here. It corresponds to an escape flux of $\sim 10^{10}$ g s^{-1}. The mean ionization lifetime of escaping hydrogen atoms is 4 hours. The model yields an atom population in a curved cometary like tail (see details in Vidal-Madjar & Lecavelier 2004).

Higher in the atmosphere, transit observations have also revealed evaporation of the hot-Jupiters closed to their parent stars. For more than ten years, transit observations allowed discoveries, detection, and characterization of extrasolar objects (Lecavelier des Etangs et al. 1995, 1997, 2005; Lecavelier des Etangs, Vidal-Madjar & Ferlet 1999; Lecavelier des Etangs 1999; Lamers et al. 1997; Nitschelm et al. 2000; Hébrard & Lecavelier des Etangs 2006; Ehrenreich et

al. 2006, 2007). In the recent discoveries, the evaporation of hot-Jupiters opens a new field of research in the exoplanet field. The field was open with the observational discovery that HD20958b is evaporating (Vidal-Madjar et al. 2003, hereafter VM03). This discovery has been challenged by a recent work of BenJaffel (2007); but the apparent discrepancy has been solved and the result obtained from this observation data set is strengthened (Vidal-Madjar et al. 2008).

In the VM03 program, three transits of HD209458b were surveyed with the STIS spectrograph on-board HST (~20 km s^{-1} resolution). For each transit, three consecutive HST orbits were scheduled such that the first orbit ended before the first contact to serve as a reference, the two following ones being partly or entirely within the transit. An average 15±4% (1σ) relative intensity drops near the center of the Lyman-α line was observed during the transits. This is larger than expected for the atmosphere of a planet occulting only ~1.5% of the star.

Because of the small distance (8.5 R_*) between the planet and the star (allowing an intense heating of the planet and its classification as a "hot Jupiter") the Roche lobe is only at 2.7 planetary radii (i.e. 3.6 R_{Jup}). Filling up this lobe with hydrogen atoms gives a maximum absorption of ~10% during planetary transits. Since a more important absorption was detected, hydrogen atoms cover a larger area corresponding to a spherical object of 4.3 R_{Jup} . Observed beyond the Roche limit, these hydrogen atoms must be escaping the planet. Independently, the spectral absorption width, with blue-shifted absorption up to -130 km s^{-1} also shows that some hydrogen atoms have large velocities relative to the planet, exceeding the escape velocity. This further confirms that hydrogen atoms must be escaping the planetary atmosphere.

The observed 15% intensity drop could only be explained if hydrogen atoms are able to reach the Roche lobe of the planet and then escape. To evaluate the amount of escaping atoms a particle simulation was built, in which hydrogen atoms are assumed to be sensitive to the stellar gravity and radiation pressure (Lecavelier des Etangs et al. 2008c; see Fig. 1). In this simulation, escaping hydrogen atoms expand in an asymmetric cometary like tail and are progressively ionized when moving away from the planet. Atoms in the evaporating coma and tail cover a large area of the star. An escape flux of $\sim 10^{10}$ g.s^{-1} is needed to explain the observations. Taking into account the tidal forces and the temperature rise expected in the upper atmosphere, theoretical evaluations are in good agreement with the observed rate (see references in Section 6).

3. Hydrodynamical escape or "Blow-off"

Four transits of HD 209458 b were then observed, again with the STIS spectrograph on board HST, but at lower resolution (Vidal-Madjar et al. 2004, hereafter VM04). The wavelength domain (1180-1710Å) includes H I as well as C I , C II , C IV , N V , O I , S I, Si III, S IV and Fe II lines. During the transits, absorptions are detected in H I , O I and C II (5±2%, 10±3.5% and 6±3%, respectively). No absorptions are detected for other lines. The 5% mean absorption over the whole H I Lyman-alpha line is consistent with the previous detection at higher resolution (VM03), because the 15% absorption covers only 1/3 of the emission line width (see discussion in Vidal-Madjar et al. 2008). The absorption depths in O I and C II show that oxygen and carbon are present

in the extended upper atmosphere of HD 209458b. These species must be carried out up to the Roche lobe and beyond, most likely in a state of hydrodynamic escape in which the escape can be described as a vertical planetary wind caring all species including the heavier species.

This picture has been strengthened by the latest HST UV observations of HD209458b performed with the new COS spectrograph on board HST. In 2009, the Atlantis Space Shuttle servicing mission has put the new spectrograph COS which is 10 to 20 times more sensitive in the UV. Observations of HD209448b transits have been carried out by France et al. (2010) and Linsky et al. (2010). Linsky et al. (2010) found an exosphere transit signature with a flux decrease by 7.8%±1.3% for the C II line at 1334.5Å and more surprisingly by 8.2%±1.4% for the Si III 1206.5Å line. These high resolution observations also show first detection of velocity structure in the expanding atmosphere of an exoplanet. Linsky et al. (2010) estimated a mass-loss rate in the range (8-40)$\times 10^{10}$ g/s, assuming that the carbon abundance is solar. This mass-loss rate estimate is consistent with previous estimates from hydrogen escape and with theoretical hydrodynamic models that include metals in the outflowing gas.

4. Observations of HD 189733 b

The observation of HD209458b transits revealed that the atmosphere of this planet is hydrodynamically escaping (Sect. 2 and 3). These observations raised the question of the evaporation state of hot-Jupiters. Is the evaporation specific to HD 209458 b or general to hot-Jupiters? What is the evaporation mechanism, and how does the escape rate depend on the planetary system characteristics? The discovery of HD 189733 b (Bouchy et al. 2005), a planet transiting a bright and nearby K0 star (V=7.7), offers the unprecedented opportunity to answer these questions. Indeed, among the stars harboring transiting planets, HD189733 presents the largest apparent brightness in Lyman-α, providing capabilities to constrain the escape rate to high accuracy.

An HST program has been developed to observed H I, C II and O I stellar emission lines to search for atmospheric absorptions during the transits of HD 189733 b (Lecavelier des Etangs et al. 2010). A transit signature in the H I Lyman-α light curve has been detected with a transit depth of 5.05±0.75%. This depth exceeds the occultation depth produced by the planetary disk alone at the 3.5σ level. This is confirmed by the analysis of the whole spectra redward of the Lyman-α line which has enough photons to show a transit signature consistent with the absorption by the planetary disk alone. Therefore, the presence of an extended exosphere of atomic hydrogen around HD 189733b producing 5% absorption of the full unresolved Lyman-α line flux shows that the planet is losing gas. The Lyman-α light curve has been fitted by a numerical simulation of escaping hydrogen to constrain the escape rate of atomic hydrogen to be between 10^9 and 10^{11} g/s, making HD 189733b the second extrasolar planet for which atmospheric evaporation has been detected (Lecavelier des Etangs et al. 2010).

These observations give new constraints for our understanding of the evaporation of hot-Jupiter because HD189733b has different characteristics than HD2095458b. It is indeed a very short period planet (P =2.2 days) orbiting a nearby late type star (K0V) with bright chromospheric

emission lines. This new detection of an evaporating planet thus provides new information on the close connection between the star and planet for these extreme planetary systems.

5. New case for detection of evaporating exosphere : Wasp-12b

Fossati et al. (2010) obtained near-UV transmission spectroscopy of the highly irradiated transiting exoplanet WASP-12b with the COS spectrograph on the Hubble Space Telescope. They detected enhanced transit depths attributable to absorption by resonance lines of metals in the exosphere of WASP-12b like absorption in the MgII λ2800Å resonance line cores. This observation suggests that the planet is surrounded by an absorbing cloud which overfills the Roche lobe and therefore must be escaping the planet.

These recent observations show that observation of evaporating exosphere is now feasible for planet transiting in front of stars fainter than HD189733b or HD209458b, possibly down to star as faint as mv$\sim$10. More importantly, this definitely shows that evaporation is a common phenomenon for Jupiter-mass planets orbiting at few stellar radii from their parent star.

6. A diagram for the evaporation status of extrasolar planets

The observational constraints given in previous sections have been used to develop a large number of models. These models aim at a better understanding of the observed escape rate and evaporation properties, and subsequently drawing the consequence on other planets and planetary systems (Lammer et al. 2003; Lecavelier des Etangs et al. 2004; Lecavelier des Etangs 2007; Baraffe et al. 2004, 2005, 2006; Yelle 2004, 2006; Jaritz et al. 2005; Tian et al. 2005; Garcia-Munoz 2007). However, all the modeling efforts lead to the conclusion that most of the EUV and X-ray input energy by the harboring star is used by the atmosphere to escape the planet's gravitational potential.

Therefore, to describe the evaporation status of the extrasolar planets, an energy diagram has been developed in which the potential energy of the planets is plotted versus the energy received by the upper atmosphere (Lecavelier des Etangs 2007). This description allows a quick estimate of both the escape rate of the atmospheric gas and the lifetime of a planet against the evaporation process. In the energy diagram, there is an evaporation-forbidden region in which a gaseous planet would evaporate in less than 5 billion years. With their observed characteristics, all extrasolar planets are found outside this evaporation-forbidden region (Fig. 2).

7. Neptune mass planets in the diagram

A plot of the mass distribution of the extrasolar planets shows that Neptune-mass and Earth-mass planets play a particular role (Lecavelier des Etangs 2007). In November 2010, with radial velocity searches, forty-six (46!) planets have been found with mass below 0.08 $M_{\rm Jup}$ (25 Earth-mass),

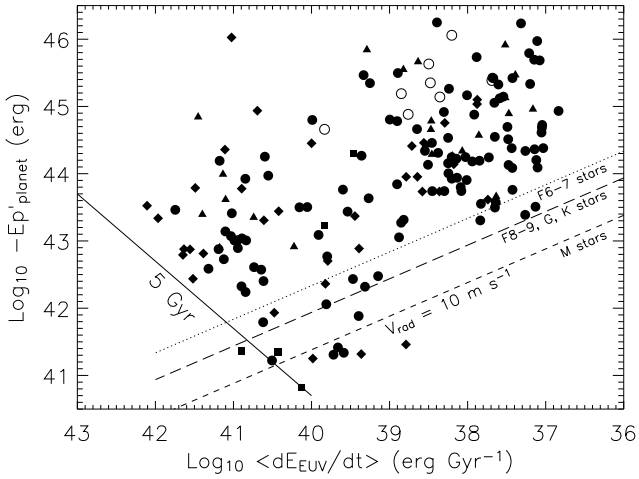

Figure 2. Plot of the potential energy of the extrasolar planets as a function of the mean EUV energy received per billion of years, $< dE_{\rm EUV}/dt >$. To keep the planets with the smallest orbital distances in the left part of the diagram, the direction of the abscissa axis is chosen with the largest value of the mean energy flux toward the left. Identified planets are plotted with symbols depending on the type of the central star: triangles for F stars, filled circles for G stars, diamonds for K stars and squares for M stars; planets orbiting class III stars are plotted with empty circles. ¿From the position in the diagram, the typical lifetime of a given planet can be rapidly extracted. If the mean energy flux $<dE_{\rm EUV}/dt>$ is given in unit of *erg per billion years*, and the potential energy is given in unit of *erg*, the simple ratio of both quantities provides the corresponding lifetime in billion of years. In the diagram, lifetime isochrones are straight lines. The lifetime of 5 Gyr is plotted with a thick line. The striking result is the absence of planets in the bottom left region which corresponds to light planets (small $-E'_p$) at short orbital distances (large $< dE_{\rm EUV}/dt >$). A plot of the lifetime line at t=5 Gyr, shows that there are no planets in this part of the diagram simply because this is an evaporation-forbidden region. Planets in this region would receive more EUV energy than needed to fill the potential well of the planet, and evaporate in less than 5 Gyr, leaving a remaining core, an evaporation remnant (also named a "chthonian" planet; Lecavelier des Etangs et al. 2004).

while only nine (9!) planets have been identified with mass in the range 0.08 $M_{\rm jup}$-0.16 $M_{\rm jup}$ (25-50 Earth-mass). This gap is not a bias in the radial velocity searches, since more massive planets are easier to detect. This reveals the different nature of these Neptune mass planets orbiting at short orbital distances. But their nature is still a matter of debate (Baraffe et al. 2005). In particular the question arises if they can be the remnants of evaporated more massive planets ("chthonian planets") as foreseen in Lecavelier des Etangs et al. (2004) ? Other possibilities include gaseous Neptune-like planets, super-Earth or ocean-planets (Kutchner 2003; Léger et al. 2004).

We plotted the position of these Neptune mass planets in the energy diagram with different hypothesis on their density (Fig. 3). We used mean planetary density of ρ_p=6 g cm^{-3} for a typical

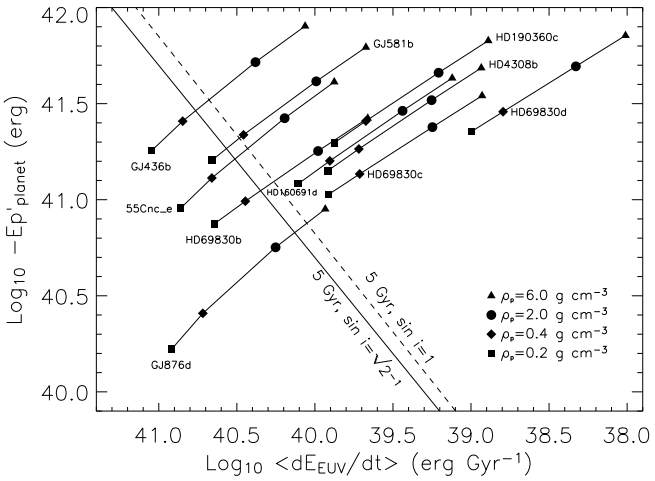

Figure 3. Plot of the potential energy of the Neptune mass planet as a function of the EUV flux for various planets' density. For GJ 581 b, GJ 436 b, HD 69830 b, 55 Cnc e and GJ 876 d, and assuming $\sin i = \sqrt{2^{-1}}$, lifetime shorter than 5 Gyr are obtained for densities below 0.28, 0.55, 0.56, 0.69 and 3.1 g cm^{-3}, respectively. If $\sin i$=1 (dotted line), the critical (minimum) densities are increased to 0.38, 0.74, 0.78, 0.93 and 4.2 g cm^{-3}, for GJ 581 b, GJ 436 b, HD 69830 b, 55 Cnc e, and GJ 876 respectively.

density of refractory-rich planets which should describe the chthonian and super-Earth planets. A lower density in the order of ρ_p=2 g cm^{-3} can be considered as more plausible for volatile-rich planets describing the ocean planets. For gas-rich planets we assumed much lower density of ρ_p=0.2 g cm^{-3} and ρ_p=0.4 g cm^{-3}, describing planets which should look more like irradiated Neptune-like planets.

GJ 876 d cannot have the density of an ocean planet and needs to be dense enough to be located above the t = 5 Gyr lifetime limit. This planet requires a density larger than 3.1 g cm^{-3} for its atmosphere to survive. GJ 876 d could be a big rocky planet, like a super-Earth, or a refractory remnant of a previous more massive planet (an evaporated ocean planet?).

In brief, the energy diagram allows us to trace three different categories for the presently identified Neptune mass planets. For half of them, the EUV input energy seems not strong enough to affect significantly these planets; we cannot conclude on their nature. For at least three other planets (GJ 436 b, 55 Cnc e and HD 69830 b), it appears that they cannot be a kind of low mass gaseous planets. With density necessarily above 0.5 g cm^{-3} to survive evaporation, these planets must contain a large fraction of solid/liquid material. Finally, GJ 876 d must be dense enough, with a density larger than ∼3 g cm^{-3}, to survive the strong EUV energy flux from its nearby parent star. This planet must contain a large fraction of massive elements (Fig. 3).

8. Conclusion

In summary, the observation of H I Lyman-α transit allows the detection of escaping atmosphere of HD 209458 b. The escape rate has been estimated through modeling of the observed transit light curve, given as estimate around $10^{10}\,\mathrm{g\,s^{-1}}$. The detection of heavy elements has then constrained the escape mechanism to be an hydrodynamical escape, or "blow-off". The evaporation processes are consistent with all measurements of the temperature profiles in the hot-Jupiter upper atmospheres with the presence of temperature rise in thermospheres. Finally, an energy diagram allows putting constraints on the density of few Hot-Neptunes. It appears that some of the low-mass planets (mass lower than ~15 Earth mass) may be evaporation remnant, or "chthonian planets" (Lecavelier des Etangs et al. 2004). Presently, the most extreme case is the planet CoRot-7b, orbiting in no more than 20 hours around a K0V type star with a semi-major axis of 0.017 AU (about 3.6 solar radius). With a mass of about 11 Earth-mass and a density of about $5\,\mathrm{g\,cm^{-3}}$ (Léger et al., 2009), this planet is very similar to what we expect for the remnant cores of former hot-Jupiters whose atmospheres have been evaporated.

References

Baraffe I., Selsis F., Chabrier G.,Allard T. S., Hauschildt P. H. Lammer H., 2004, A&A, 419, L13
Baraffe I., Chabrier G., Barman T. S., Selsis F., Allard F., Hauschildt P. H., 2005, A&A, 436, L47
Baraffe I., Alibert Y., Chabrier G., Benz W., 2006, A&A, 450, 1221
Ben-Jaffel L., 2007, ApJ, 671, L61
Bouchy F., et al., 2005, A&A, 444, L15
Désert J.-M., Vidal-Madjar A., Lecavelier Des Etangs A., Sing D., Ehrenreich D., Hébrard G., Ferlet R., 2008, A&A, 492, 585
Ehrenreich D., Tinetti G., Lecavelier des Etangs A., Vidal-Madjar A., Selsis F., 2006, A&A, 448, 379
Ehrenreich D., Hébrard G., Lecavelier des Etangs A., Sing D. K., Désert J.-M., Bouchy F., Ferlet R., Vidal-Madjar A., 2007, ApJ, 668, L179
Fossati L., et al., 2010, ApJ, 720, 872
France K., Stocke J. T., Yang H., Linsky J. L., Wolven B. C., Froning C. S., Green J. C., Osterman S. N., 2010, ApJ, 712, 1277,
García M. A., 2007, Planetary & Space Science, 55, 1426
Hébrard G., Lecavelier des Etangs A., 2006, A&A, 445, 341
Jaritz G. F., Endler S., Langmayr D., Lammer H., Grießmeier J.-M., Erkaev N. V., Biernat H. K., 2005, A&A, 439, 771
Kuchner M. J., 2003, ApJ, 596, L105
Lamers H. J. G. L. M., Lecavelier Des Etangs A., Vidal-Madjar A., 1997, A&A, 328, 321
Lammer H., Selsis F., Ribas I., Guinan E. F., Bauer S. J., Weiss W. W., 2003, ApJ, 598, L121
Lecavelier des Etangs A., 1999, A&AS, 140, 15
Lecavelier des Etangs A., 2007, A&A, 461, 1185
Lecavelier des Etangs A., Deleuil M., Vidal-Madjar A., Ferlet R., Nitschelm C., Nicolet B., Lagrange-Henri A. M., 1995, A&A, 299, 557
Lecavelier des Etangs A., Vidal-Madjar A., Burki G., Lamers H. J. G. L. M., Ferlet R., Nitschelm C., Sevre F., 1997, A&A, 328, 311
Lecavelier des Etangs A., Vidal-Madjar A., Ferlet R., 1999, A&A, 343, 916

Lecavelier des Etangs A., Vidal-Madjar A., Hébrard G., McConnell J., 2004, A&A, 418, L1
Lecavelier des Etangs A., Nitschelm C., Olsen E. H., Vidal-Madjar A., Ferlet R., 2005, A&A, 439, 571
Lecavelier des Etangs A., Pont F., Vidal-Madjar A., Sing D., 2008a, A&A, 481, L83
Lecavelier des Etangs A., Vidal-Madjar A., Desert J.-M., Sing D., 2008b, A&A, 485, 865
Lecavelier des Etangs A., Vidal-Madjar A., Desert J.-M., 2008c, Nature, 456, E1
Lecavelier des Etangs A., et al., 2010, A&A, 514, A72
Léger A., et al., 2004, Icarus, 169, 499
Léger A., et al., 2009, A&A, 506, 287
Linsky J. L., Yang H., France K.,Froning C. S., Green J. C., Stocke J. T., Osterman S. N., 2010, ApJ, 717, 1291,
Nitschelm C., Lecavelier des Etangs A., Vidal-Madjar A., Ferlet R., Olsen E. H., Dennefeld M., 2000, A&AS, 145, 275
Sing D. K., Vidal-Madjar A., Desert J.-M., Lecavelier des Etangs A., Ballester G., 2008a, ApJ, 686, 658
Sing D. K., Vidal-Madjar A., Lecavelier des Etangs A., Désert J.-M., Ballester G., Ehrenreich D., 2008b, ApJ, 686, 667
Tian F., Toon O. B., Pavlov A. A., De Sterck H., 2005, ApJ, 621, 1049
Vidal-Madjar A., Lecavelier des Etangs A., Désert J.-M., Ballester G. E., Ferlet R., Hébrard G., Mayor M., 2003, Nature, 422, 143 (VM03)
Vidal-Madjar A., Lecavelier des Etangs A., 2004, ASP Conf. Ser., 321, 152
Vidal-Madjar A., et al., 2004, ApJ, 604, L69 (VM04)
Vidal-Madjar A., Lecavelier des Etangs A., Désert J.-M., Ballester G. E., Ferlet R., Hébrard G., Mayor M., 2008, ApJ, 676, 57
Vidal-Madjar A., Sing D. K., Lecavelier des Etangs A., et al. 2011, A&A, in press
Yelle R. V., 2004, Icarus, 170, 167
Yelle R. V., 2006, Icarus, 183, 508